LIQUID STATE: BETWEEN TWO CRITICAL ANOMALIES?

A.Voronel

R.&B.Sackler School of Physics & Astronomy,

Tel-Aviv University, 69978, Tel-Aviv, Israel

Limits of the liquid state's existence are considered relative to the form of an interatomic potential curve. Transport coefficients at high temperature have been found to follow a modified "corresponding states law". At the low temperature region, however, liquid's behavior is material dependent. A decrease of freezing temperature (in a reduced scale) in any melt leads to enhancement of C_p anomaly similar to that of water at its super-cooled state. The fluctuations of entropy in any super-cooled liquid lead to emerging of clusters with relatively shorter attraction part of their potential well. This forms a reason for an existence of a metastable critical point of "liquid-vapor" type for clusters. This virtual critical point has to be situated well below the glass point and produce a cause for another universality in liquids' behavior. The vitrification point is determined by kinetic, material dependent, reasons and has no straightforward relation to the virtual lower critical point.

The range of the liquid state of matter is rather limited in both density and temperature:

$$1< D/D_c < 2.6 – 4.2 \qquad (1)$$

$$1> T/T_c > 0.15 – 0.8\ (1) \qquad (2)$$

Here D_c and T_c are the critical density and temperature correspondingly. 1 in parenthesis of inequality (2) means that some matters have no liquid state at all.

Although the "Corresponding States Law" for thermodynamic properties of liquids does not work in a simplified form which follows from the van der Waals equation, it is still valid more or less close to the liquid-vapor critical point (Fig.1). This point can be identified by singularities of both thermodynamic and kinetic properties (Fig.2 [1]).

These singularities may be expressed by universal formulae in reduced coordinates $t=(T-T_c)/T_c$, $d=(D-D_c)/D_c$. The closer to the critical point the more accurate are these asymptotic formulae. However, even with deviations from the universality the reduced coordinates allow to compare the properties of matters in a common scale and to reveal their both similarities and differences.

Unfortunately, it is not always easy to do because of experimental difficulties with the critical points, in particular, for the transport properties of glass forming liquids and ionic melts. Nevertheless, a correctly written Arrhenius equation for resistivity gives a desired "corresponding states law" for all the ionic melts and solutions [2]:

$$\rho/T = A \exp (E_r/T) \qquad (3)$$

An usual range of measurements in the liquid state for the most of melts is located between E_r/T being equal to 3 and 5 – 6. The range of universality (see Fig.3a) breaks at about $E_r/T > 5$ (see inequality (2)), more or less close to the melting points of liquids.

The observed universal temperature dependence of resistivity provokes a desire to check up also a viscosity behavior. One can see in Fig.3b the analogous picture (and analogous formula with roughly the same range of universality):

$$\eta/T = B \exp (E_v/T) \qquad (4)$$

The energy values E_r and E_v are different. While E_r is slightly less than an estimated T_c of a corresponding melt, E_v usually exceeds it. Since the difference is not great the scale E/T does not much differ from the reduced scale of the Fig.1.

One may conclude from the Fig.3 that while in a high temperature range the general approach to the liquid state is justified, in the low temperature limit (freezing or vitrification) liquids demonstrate individual behavior depending on details of interaction between their particles. This is not exactly true. Let us consider in detail the liquid's behavior on cooling (and super-cooling).

There is no expected singularity in melting point but there is a rule (confirmed by simulations for hard spheres) which puts a limit for an amplitude of atomic vibration in crystalline lattice, so named, Lindemann Criterion of Melting. The criterion states that if a dimensionless ratio $<X^2(T)>$ of the mean square vibrational displacement of particles (measured, for instance, through the Debye-Waller factor) from their nominal lattice positions (related to the nearest neighbor distance a) exceeds a characteristic value L, a long range order of the crystal is destroyed. The L varies with crystal structure (it is roughly 0.013 for FCC and close to 0.022 for BCC crystals [3])

As one may see from the Fig 1 the melting for different liquids takes place at a rather different reduced temperature. How both critical and melting points depend on a liquid's interaction potential?

The computer simulation [4] has revealed (Fig.4) that the existence range of the liquid state is determined by an attractive part the potential. The shorter is this part the lesser is the distance between the critical and melting points. A depth of the potential well roughly corresponds to the critical temperature and the long range attractive forces cause the position of a fusion within the well. The fusion takes place when the amplitude of vibration (by other words, uncertainty of the position) reaches its limit (see Fig.5). For the fusion not an energy is important but the uncertainty of atomic positions. Thus the melting point is determined by the width of the well, not by its depth This explains the difference between the noble gas and alkali metal in Fig.1

Has one another way (other than heating) to increase the uncertainty of atomic positions, e.g. the mean square displacement $<X^2(T)>$? One can mix atoms of different size in one lattice to introduce a controllable amount of disorder. Cooling down, for instance, the fifty-fifty mixture of alkali metals (Fig.6 [3]) one can freeze it in one point and form a mixed lattice with an average lattice parameter. Thus in this case the total mean square relative variation of inter-atomic distance (also can be measured through the Debye-Waller factor) consists from the two terms:

$$<X_t^2(T)> = <X_s^2> + <X_v^2(T)>, \qquad (5)$$

where the relative dispersion of atomic size $<X_s^2> = (\Delta a)^2 / <a^2> = p(1-p)(a_1-a_2)^2/<a^2>$, p is a concentration. The mixture's individual characteristics $<X_s^2>$ does not depend on temperature. $<X_v^2(T)>$ - the vibrational displacement of centers of atoms from their positions. If one assumes this generalized Lindemann criterion working for mixed crystals the $<X_t^2>$ has to be equal just to the same fixed number L. Using Debye theory

for vibrations at high temperature ($T > \theta_D$) one may rewrite the equation (5) for melting point:

$$T_m = T^*\{1- <X_s^2> / L\}, \qquad (6)$$

where T* is the melting temperature of a perfect virtual lattice with average atomic parameters. Thus the term $<X_s^2>/ L$ is a reduction factor proportional to a built-in relative disorder. The eq.(6) works extremely well for alloys and solid solutions of ionic crystals [5] (if only the components have a similar symmetry) and also can be easily generalized for multi-component systems. Since the melting temperature may hardly become negative an amount of static disorder $<X_s^2>$ in any real crystalline structure is limited. It gives a rather realistic prediction of phase diagrams [5] including a phase separation (eutectics) for a too great size disparity (the Hume-Rothery rule). Since many glasses are actually super-cooled eutectics let us pay a particular attention to this way to reduce the melting point.

Even the pure alkali metals close to their freezing points have a slight enhancement of their specific heat from the liquid side [6]. This enhancement becomes more pronounced when the relative temperature of freezing has been driven down as one can see from Fig.7. The relative role of the two parts of eq. (5) changes correspondingly. All the dynamical processes are slowing down and the term $<X_v^2(T)>$ becomes comparatively small. This is fully compatible with the enhancement of the heat capacity C_p, e.g. growth of entropy fluctuations (since $C_p = <(\Delta S)^2>$). The similar enhancement was observed also in super-cooled water [7, 8] and recently found to be a precursor of a kind of critical point [9] (interpreted as “liquid-liquid”, see Fig.8).

Let us turn back to the Fig.4. It was shown by computer simulation [4] that if the

effective range of attractive force was shorter than roughly 30% of an interatomic distance the critical point appeared below the sublimation line. Does it mean the criticality disappears? No, it becomes metastable (see Fig.9 C). It does mean for a substance with very short-ranged attractive forces the critical point still can be realized (under the condition that a crystallization has somehow been avoided [4]) deeply below the freezing point.

One hardly can vary an interaction potential between atoms. But people are able to vary a ratio between a range of the intermolecular attractive force and a diameter of a particle (Fig.10) and thus to shorten the relative range of the force by varying the diameter. A striking example of this is a phase diagram of molecule C_{60} [10] which exhibits its critical point very close to its triple point ($T_m/T_c \cong 1$).

This possibility has also been experimentally realized in mixtures of spherical colloidal particles and non-adsorbing polymers, where the range of the attractive branch of the effective colloid-colloid interaction has been varied by changing the size of the polymer [11]. Experiment, theory and simulation all suggest that when the width of the attractive part of a potential well becomes less than about one third of the diameter of the colloidal spheres, the colloidal liquid phase disappears. As the range of attraction decreases, the "liquid-vapor" coexistence moves into the metastable regime. This also means that the compressibility of the corresponding fluid near the metastable critical point is increasing and the resulting fluctuations of density occur. Large amorphous clusters (more than 100 particles – see Fig.11 [4]) near the critical point have been observed in the time scale shorter than necessary for the crystallization from a metastable state.

In the Fig.3 the transport coefficients of glass forming liquids have been presented.

One can see that all of them at their high temperature region behave universally in good agreement with the Arrhenius formula. It means the corresponding process may be roughly reduced to a series of uncorrelated elementary events with the corresponding average activation energy. This is possible until the average energy of a particle is high enough to maintain a noticeable probability to leave their cage. However, all the melts (as well as other liquids) in their super-cooled state strongly deviate from this way and the deviations are material dependent. It is natural to assume that at low temperature the attractive forces lead to stochastically emerging associates (clusters) which impede the uncorrelated motions of individual particles. And more particles are never able to leave their cages. Though this trend is, probably, the universal feature, the rate of clusters' growth depends on the details of a potential well.

The key idea that makes a ground stone of many recent theories of molecular dynamics of super-cooled systems is the concept of a sort of heterogeneity including also a spatial inhomogeneity in nano-metric scale [12,13,14]. Some authors [13,15] connect these inhomogeneities with the sort of order parameter fluctuations. Thus at low temperature we again are welcomed to the criticality! Probably the lower critical point suggested in water [9] is not a particular feature of water, but rather a general phenomenon?

Whatever is the reason for emerging a heterogeneity in super-cooled liquids, the corresponding medium on its mesoscopic (nano-metric) scale may be presented as a composite material with inclusions (clusters) of greater rigidity which live much longer than a relaxation time of an individual molecule. (It can be also understood from the analysis of, so named, "Translation-Rotation Paradox" [16]). Thus an effective conductivity of such a composite consisting of two phases of different conductivity

(suppose one of them to be an insulator) for a first approximation ("Effective Medium Approximation" - EMA) may be presented as:

$$\sigma_{eff} = \sigma_1 \{1 - P_2(T)/P'_c\} \qquad (7)$$

Here σ_{eff} is a measured quantity, σ_1 – the conductivity of a fluid phase and P_2 – a volume fraction of a rigid phase (clusters) which depends on both thermodynamic condition and physico-chemical properties of the substance. The EMA actually works for $P_2 << 1$ only and P_c is a treshold dependent on a geometry of the composite structure (see for instance Fig.12 and compare with Fig.14 [17]). For high P_2 closer to the treshold value the right side of the eq.(7) transforms into a complicated function of the inner structure of the material. The analogous formula may be written also for fluidity $\varphi = 1/\eta$ [18]:

$$\varphi_{eff} = \varphi_1 \{1 - P_2(T)/P''_c\} \qquad (8)$$

The Pc in eq.(7) and (8) is essentially different since the cluster which blocks completely a mechanical movement (Fig.12) may only slightly interfere with an electrical current.

Until the term P_2/P_c (a collective obstruction effect of the clusters) is small the relation between the conductivity and fluidity is weakly dependent on temperature range and determined mostly by the high temperature (universal) behavior of liquids (Fig.3c [19]). However, when the treshold for the rigid phase is approached, e.g. the concentration of clusters can not be considered small anymore, the function $P_2(T)/P_c$ determines both viscous and conductive behavior (though rather differently) and the next approximations are necessary [20]. The number of clusters and their life span are growing with cooling. It has to cause an enhancement of C_p analogous to that of water [9] and alkali metals [7].

Indeed, an anomaly of C_p close to a glass point is a common feature of glass forming liquids better pronounced for the fragile glasses (Fig.13 [21]). One can dare to assume that this anomaly is of a general nature, the same (or similar) as the one mentioned above.

Let us recollect now what has been said above about the metastable liquid-vapor critical point. The long living clusters emerge as a result of fluctuations close to this point (Fig.11) both below and above the sublimation line. The series of recent computer simulations of super-cooled fluid [17] explicitely reproduce a heterogeneity which implies an existence of multi-molecular clusters (Fig.14) moving collectively during a long time (relatively to an individual molecule relaxation time). Thus the clusters of different configurations appear in super-cooled liquid. An attractive branch of an interaction potential between these clusters appear to be much shorter in comparison with their diameter in accordance with Fig.10. The concentration of these clusters is growing with cooling and the system is driven to the critical point of the kind which has been observed in colloidal systems [11]. The difference is that both size and concentration of these clusters depend on thermodynamic parameters of the system as a whole. In the real liquids in their super-cooled state all the dynamic processes dramatically slow down and a rough surface friction between clusters interlocks any macroscopic flow in T_g much earlier than the critical phenomena are fully developed.

Nevertheless, the microscopic motions (diffusion, conductance, aging) below the glass point are still allowed. How far from this virtual critical point T_v the glassification really stops the rearrangement of clusters depends on details of a form of molecules and inter-action between them. So named, “fragile” [21] glasses are, probably, those with more symmetric molecules, which makes them to be frozen lower (closer to the T_v point).

Some information on interrelation between the microscopic and macroscopic motions can be obtained from a diffusion-viscosity (or conductivity-viscosity) correlation (see Fig.3c and 15). Experiments with probe molecules of different size [15, 22], translational and rotational diffusion measurements [15, 23] give an information on size and concentration of clusters. Precise measurements of density together with viscosity [24] allow both to see the enhancement of compressibility (which may be accepted as the signature of the virtual critical point' proximity) and to calculate the total volume fraction of clusters in a super-cooled liquid as a function of temperature (Fig.16 [25]).

Let us formulate again our hypothesis: At the low reduced temperature the "gas" of clusters emerging in a super-cooled liquid should approach its metastable "liquid-vapor" critical point. (Since the average density in this point is high one may name it also a "liquid-liquid" point as it has been done in [9]). Although in [9] this phenomenon looks as a particular feature of water, it can be generalized for other polyamorphic liquids, which form orientation-dependent intermolecular bonds, like SiO_2, GeO_2 [27] and a wide class of liquids with a core-softened potential [27, 9]. More probably, this is an universal phenomenon since the collective interaction of molecules always produces not one but a variety of local minima of thermodynamic potential in a super-cooled fluid. A quasi-pair potential of the collective interaction in disordered (or partially ordered) clusters consequently includes more than one minimum and thus leaves possibilities for more than only one configuration. Even the interaction between Ar atoms in a reasonably big cluster is not absolutely spherically symmetric and includes the orientation-dependent bonds (which makes argon crystals to be of FCC structure instead of HCP).

Thus a coexistence of high density and low density phases producing a metastable critical point may lay beneath the T_g of all the glass forming liquids even without such specific features as hydrogen bonds [9] or core collapse [27]. In usual physical experiment so far one hardly is able to control the thermodynamic path of measurements in this range. That's why only a weak influence of this critical point is usually observed.

The slowing down of the kinetics at the low reduced temperature puts the limit of ergodicity on all the systems in their glass point. This point T_g has no straightforward relation to the metastable critical point T_v and depends on the geometry of the clusters. The classification of "strong" and "fragile" glasses (Fig.13 [21]) characterizes how far from the lower situated virtual critical point T_v these liquids reach the limit where a hydrodynamic motion is interlocked. The strong glasses vitrify so far from the T_v that the signature of it hardly appears in anomalies of their thermodynamic functions.

REFERENCES:

[1] A.Voronel, "Phase Transitions and Critical Phenomena", v.5b, 343, ed. by C.Domb and M.Green, Academic Press, Oxford, 1976.

[2] A.Voronel, V.Machavariani et al.,Journ.Phys.: Cond.Matt., **11**, 8773, (1999).

[3] A.Voronel et al., Phys.Rev.Lett., **60**, 2402, (1988)

[4] G.Vliegenthart, H.Lekkerkerker, Physica **A263**, 378, (1999).

[5] S.Rabinovich, A.Voronel, L.Peretzman, Journ.Phys. C: Sol.St.Phys., **21**, 5943, (1988). D.Berreby, A.Voronel et al. J.Phys: Cond.Matt., **4**, 10139, (1992).

[6] A.Voronel, V.Steinberg, T.Sverbilova, Phys.Lett., **79A**, 180, (1980).

[7] M.Anisimov, A.Voronel et al., Pis'ma ZhETF, **15**, 449, (1972)

[8] R.Speedy, C.Angell, Journ.Chem.Phys., **65**, 851, (1976).

[9] O.Mishima, H.E.Stanley, Nature, **392**, 164, (1998). M.Reza Sadr-Lahijany, H.E. Stanley et al., Phys.Rev.Lett., **81**,4895, (1998).

[10] M.Hagen et al., Nature, **365**, 425, (1993).

[11] D.Frenkel, Physica **A263**, 26, (1999).

[12] I.Chang et al., Journ.Non-Cryst.Sol., **172-174**, 248, (1994).

[13] E.Fisher et al. Phys.Rev.Lett., **68**, 2344, (1992).

[14] M.Cicerone, M.Ediger, Jour.Phys.Chem., **97**,10489,(1993). Journ.Chem.Phys.,**102**,471,(1995). *Ibid.*, **104**, 7210, (1996).

[15] S.Kivelson et al., Journ.Chem.Phys., **101**,2391, (1994).

[16] F.Stillinger, J.Hodgdon, Phys.Rev**. E 50**, 2064, (1994).

[17] C.Donati, J.Douglass et al., Phys.Rev.Lett., **80**, 2338, (1998). S.Glotzer, C.Donati,, Journ.Phys.: Cond.Matt., **11**, A285, (1999).

[18] Y.Navot, M.Schwartz, Phys.Rev.Lett., **79**, 4786, (1997).

[19] A.Voronel, V.Machavariani et al., Phys.Rev.Lett., **80**, 2630, (1998).

[20] E.Garboczi, J.Douglass, Phys.Rev. **E 53**, 6169, (1996). J.Douglass,Journ.Phys.:Cond.Matt.**11**, A329, (1999).

[21] C.A.Angell, Science, **267**, 1924, (1995)

[22] K.L.Ngai et al., Macromolecules, **21**, 3030, (1998).

[23] A.Kisliuk, D.Quitmann, A.Voronel et al., Phys.Rev. **B 52**, 13083, (1995).

[24] W.Hasz, C.T.Moynihan et al., Journ.Non-Cryst.Sol., **161**, 127, (1993).

[25] V.Machavariani, A.Voronel, Phys.Rev. **E 61**, 2121, (2000).

[26] C.Roberts, P.Debenedetti et al., Phys.Rev., **77**, 4386, (1996).

[27] P.Hemmer, G.Stell, Phys.Rev.Lett. **24**,1284, (1970).

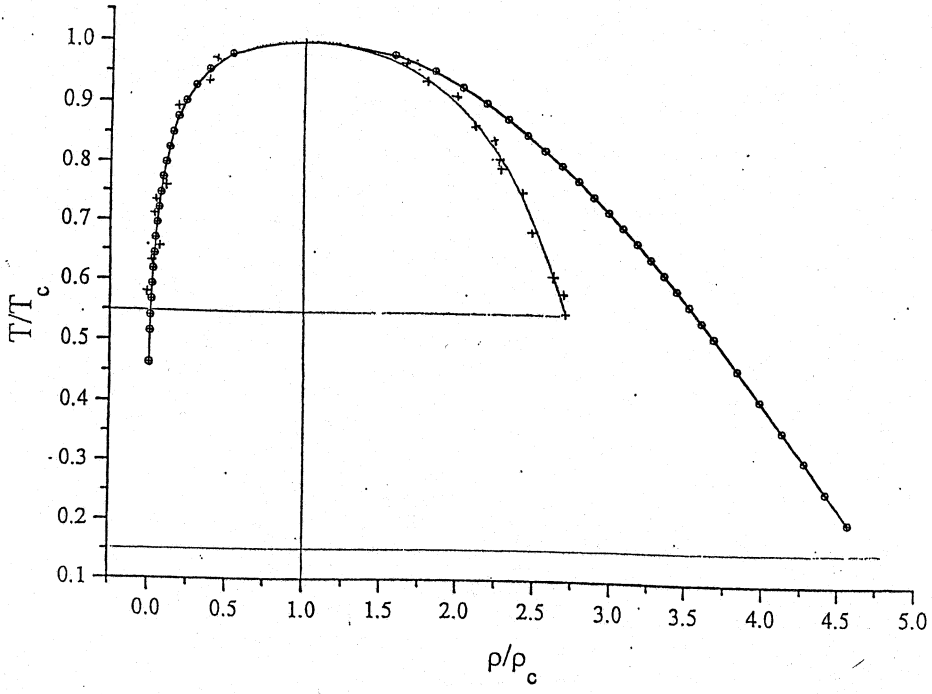

Fig. 1 Liquid - vapor coexistance curve for different substances in reduced coordinates: (+)-Ar, (o) - Cs

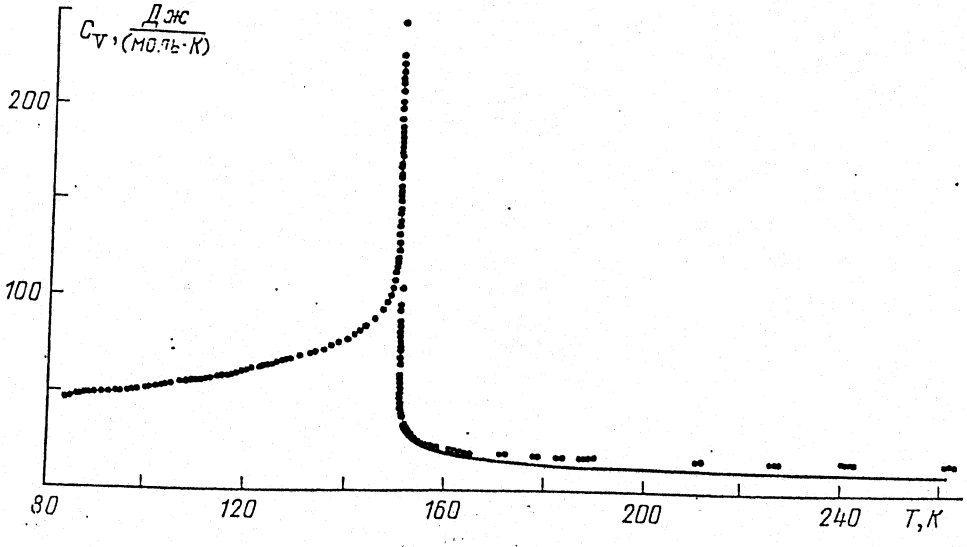

Fig. 2 Isochoric heat capacity of a substance around critical point: (.)-Ar, - asymptotic universal curve

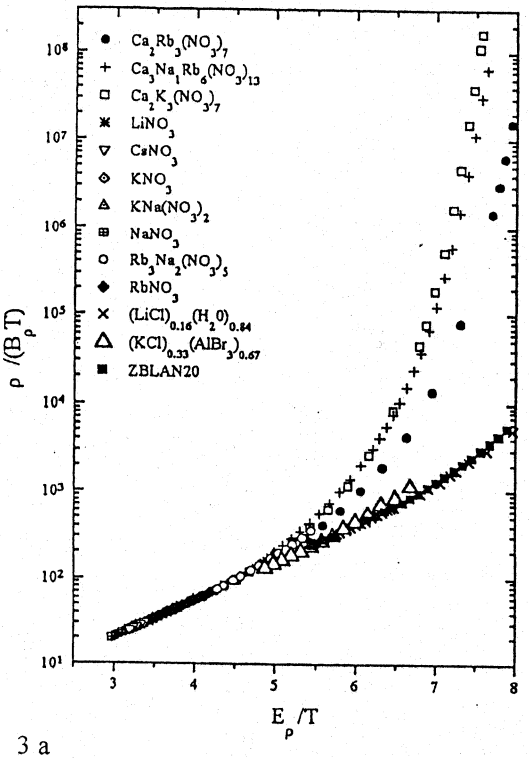

3 a

Reduced resistivity of ionic melts as a function of reduced temperature ("Arrhenius plot").

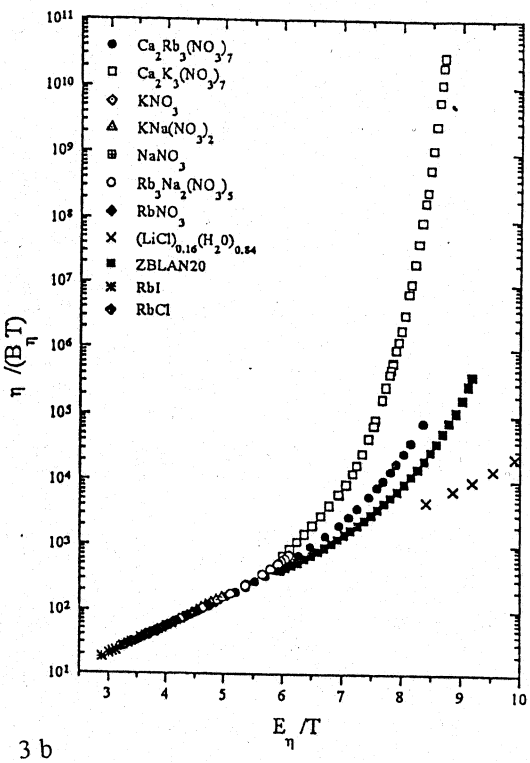

3 b

Reduced viscosity of ionic melts as a function of reduced temperature ("Arrhenius plot").

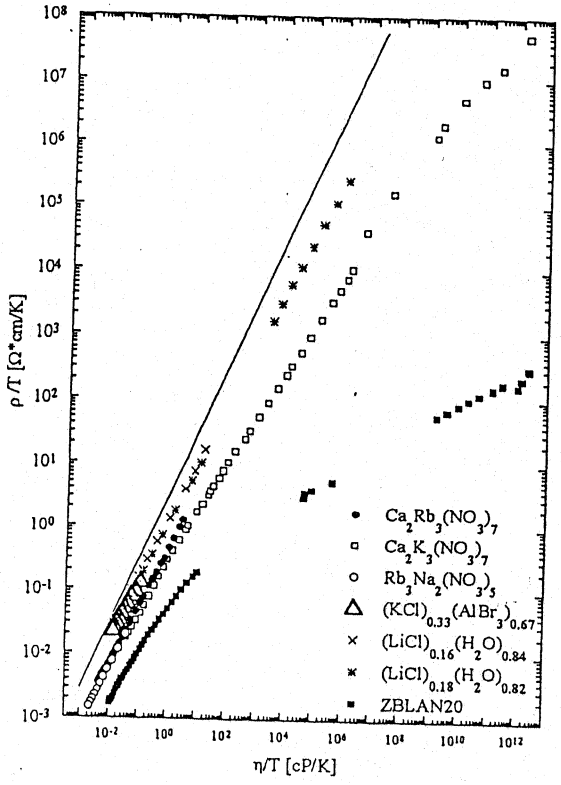

3 c

ρ/T as a function of η/T in a log-log plot for ionic melts and solutions. The solid line corresponds to the slope *m* equals to 1 (Stokes-Einstein Behavior).

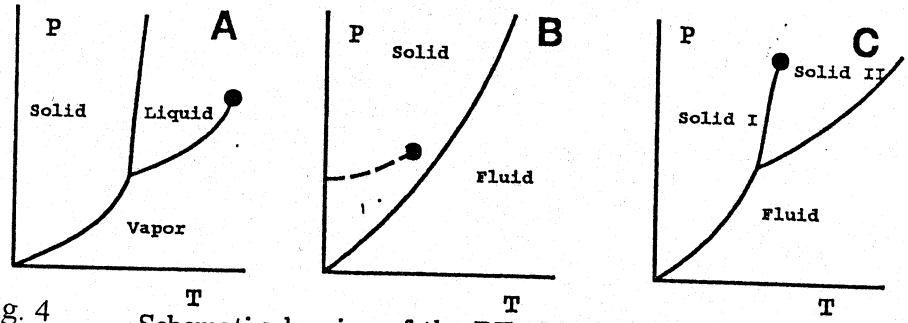

Fig. 4 Schematic drawing of the PT phase diagram of a system of spherical particles with (A): an attractive interaction with a range larger than one third of the hard-core diameter. (B): range of attractive interaction between 5 and 20 % of the hard-core diameter. (C) range of the attractive interaction less than 5% of the hard-core diameter.

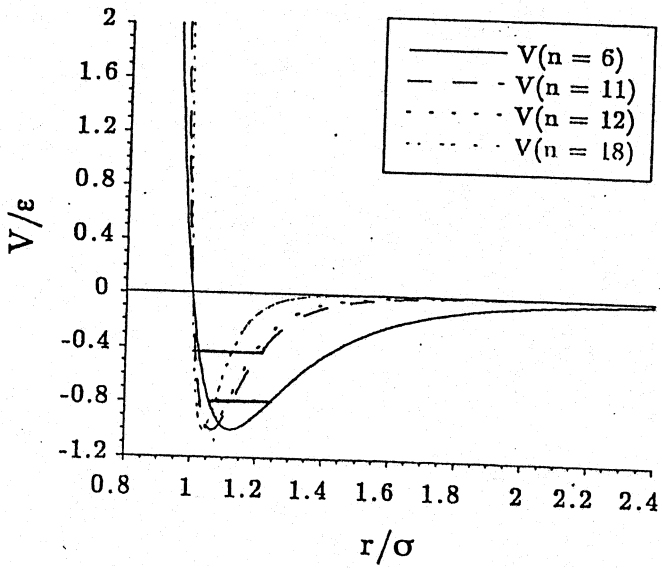

Fig. 5 The potential energy as function of the distance between the particles.

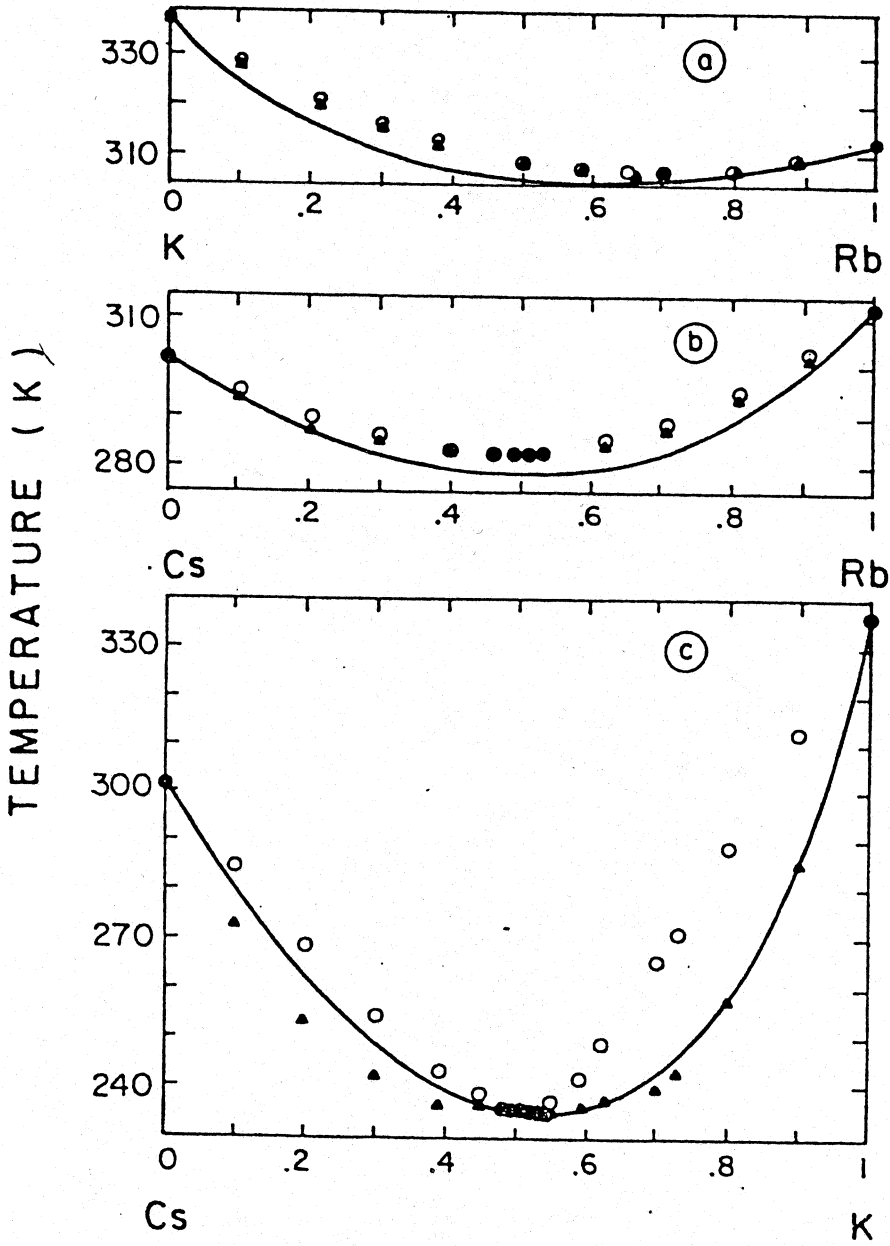

Fig. 6 Diagrams of state of alkali-metal mixtures. The two kinds of points are experimental data (Ref. 1) on freezing and melting temperatures of alloys at corresponding concentrations. The lines are our calculation in accordance with Eq. (4).

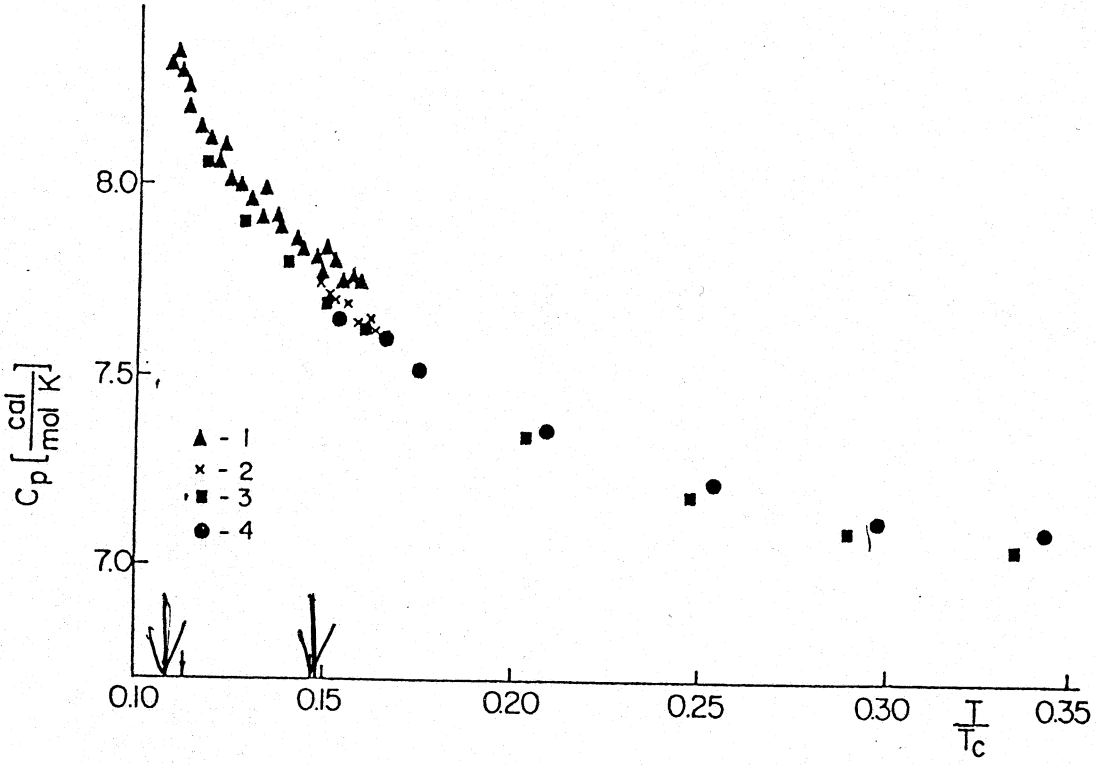

Fig. 7 Specific heat of the alkalis and their mixtures as a function of the reduced temperature T/T_c. (1) K–Cs (our measurements), (2) Cs (our measurements), (3) Na–K [8], (4) K [8].

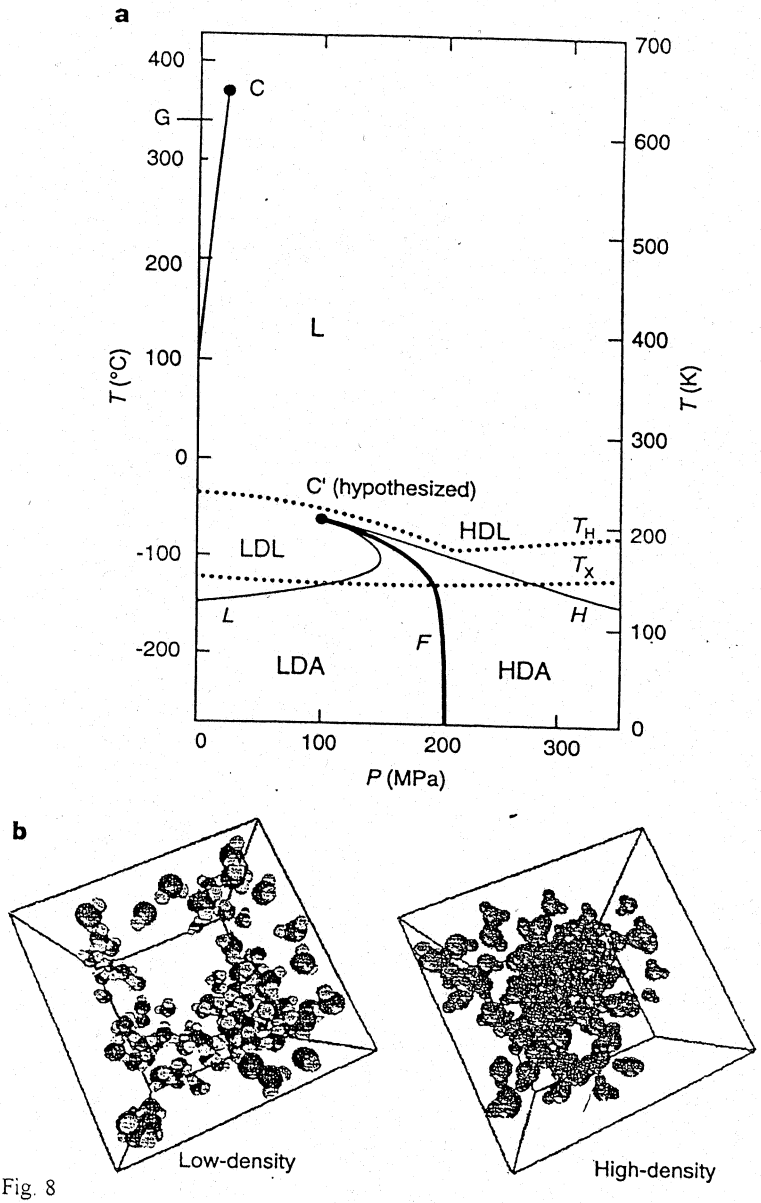

Fig. 8

Detailed version of the projection onto the P–T plane of the equilibrium $V = V(P, T)$ surface of water **a**, The phase relations between liquid water, LDL, HDL, LDA and HDA: C and C′ denote the known critical point and the hypothesized 'second' critical points respectively, F denotes the line of first-order phase transitions that emanates from C′ and separates the high-density and low-density phases that occur for temperatures below $T_{c'}$. The curves denoted L and H are the limits of metastability of the HDA and LDA phases, respectively. **b**, Molecular-dynamics 'snapshots' of LDL and HDL, coexisting and separating in liquid water. The subset of water molecules identified in the left panel have a smaller local density than the average, while those shown in the right panel have a larger local density.

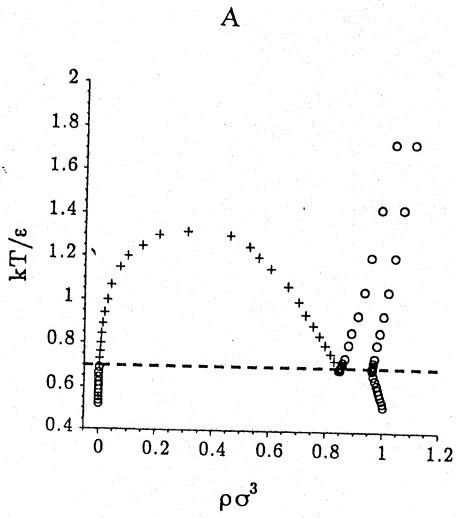

Fig. 9

Phase diagrams for n = 6 (A)

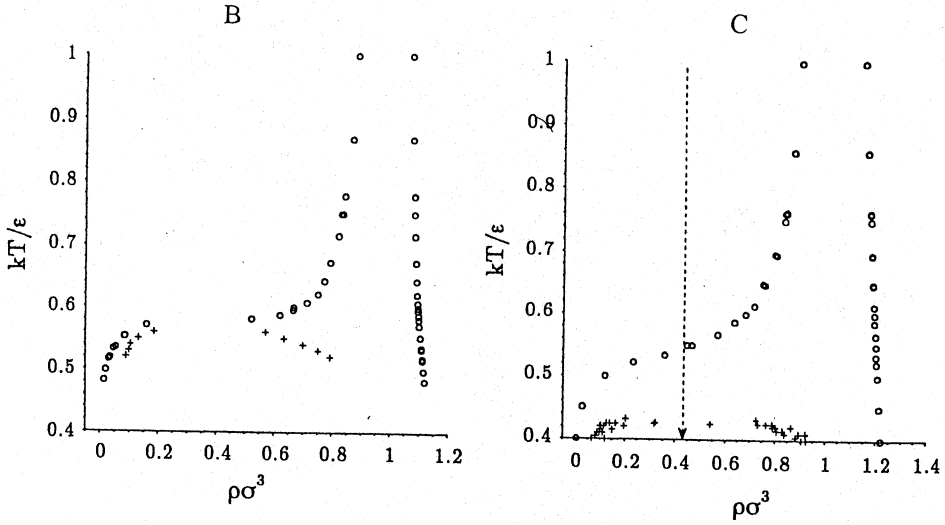

Phase diagrams for n = 12 (B) and n = 18 (C). For n = 12 the critical temperature is 0.56 and the critical density is 0.43. For n = 18 the critical temperature is 0.43 and the critical density is 0.43.

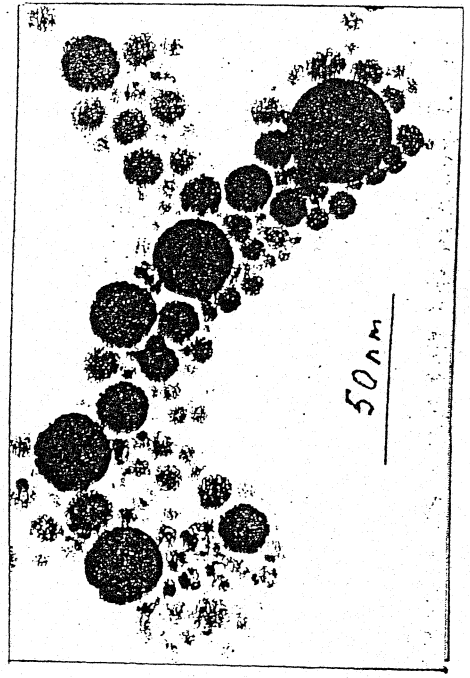

Nanospheres of alumina in paraffin

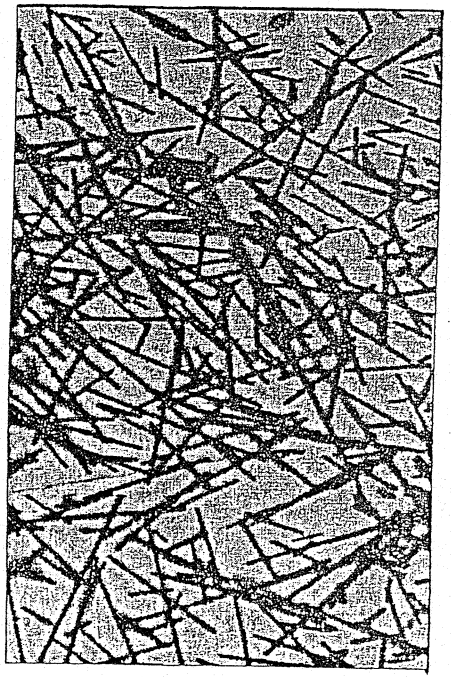

Carbon fibers in paraffin.

Fig. 12

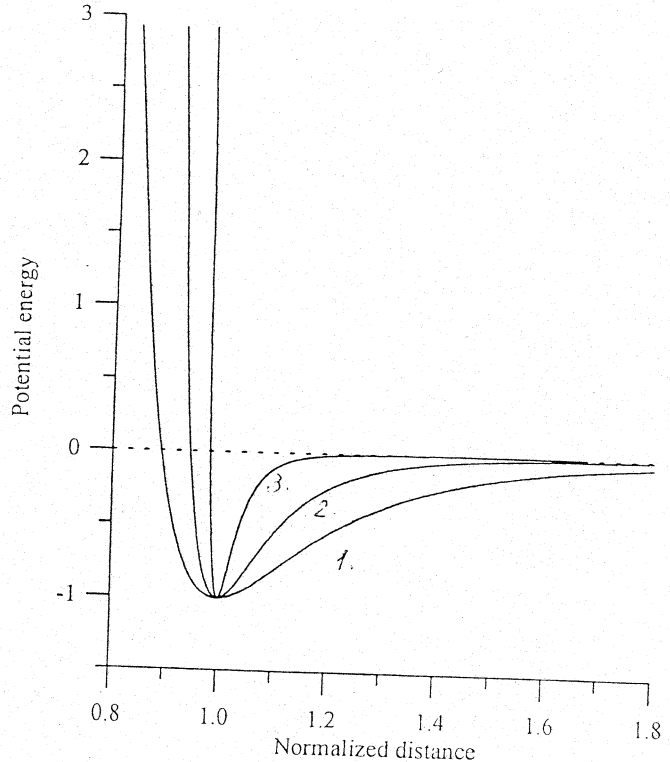

Fig.10 Potential energy as a function of normalized distance between particles/clusters L=r/(ℓ+R)
1. ℓ= 0; 2. ℓ= 1R ; 3. ℓ= 5R.

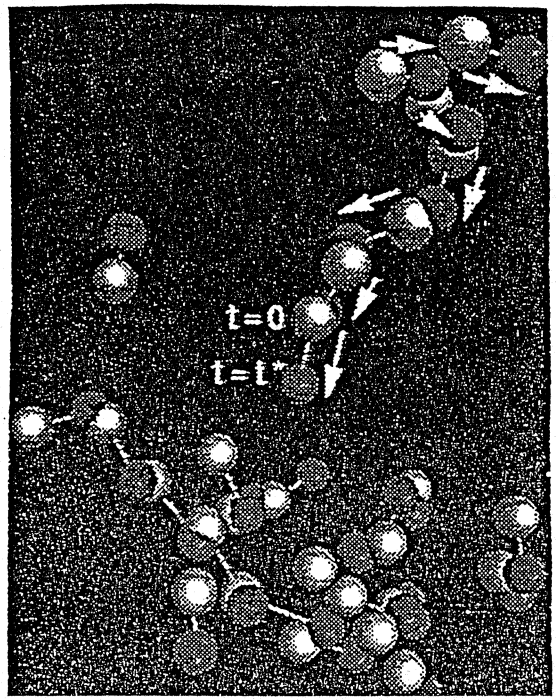

Fig. 14

Mobile particles in a subregion of the simulation box at two different times. Light spheres: particles at t=0. Dark spheres: same particles at a later time.

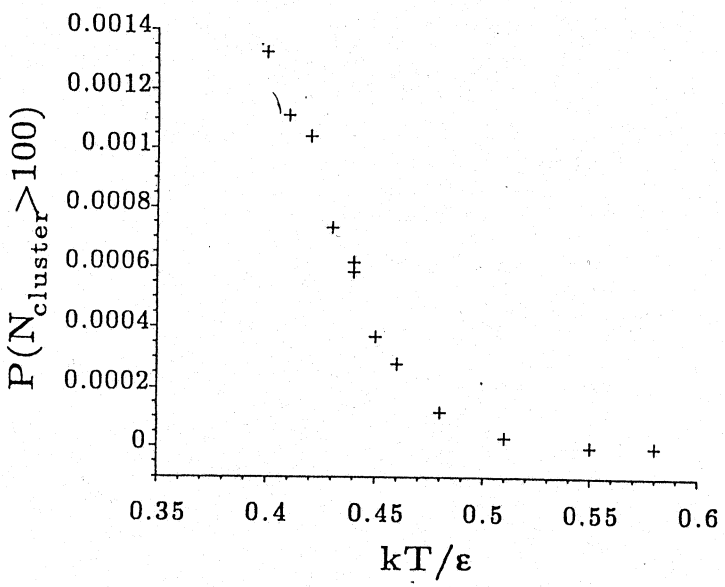

Fig. 11

Probability of clusters with more then 100 particles versus the temperature for the case of Fig. 9c.

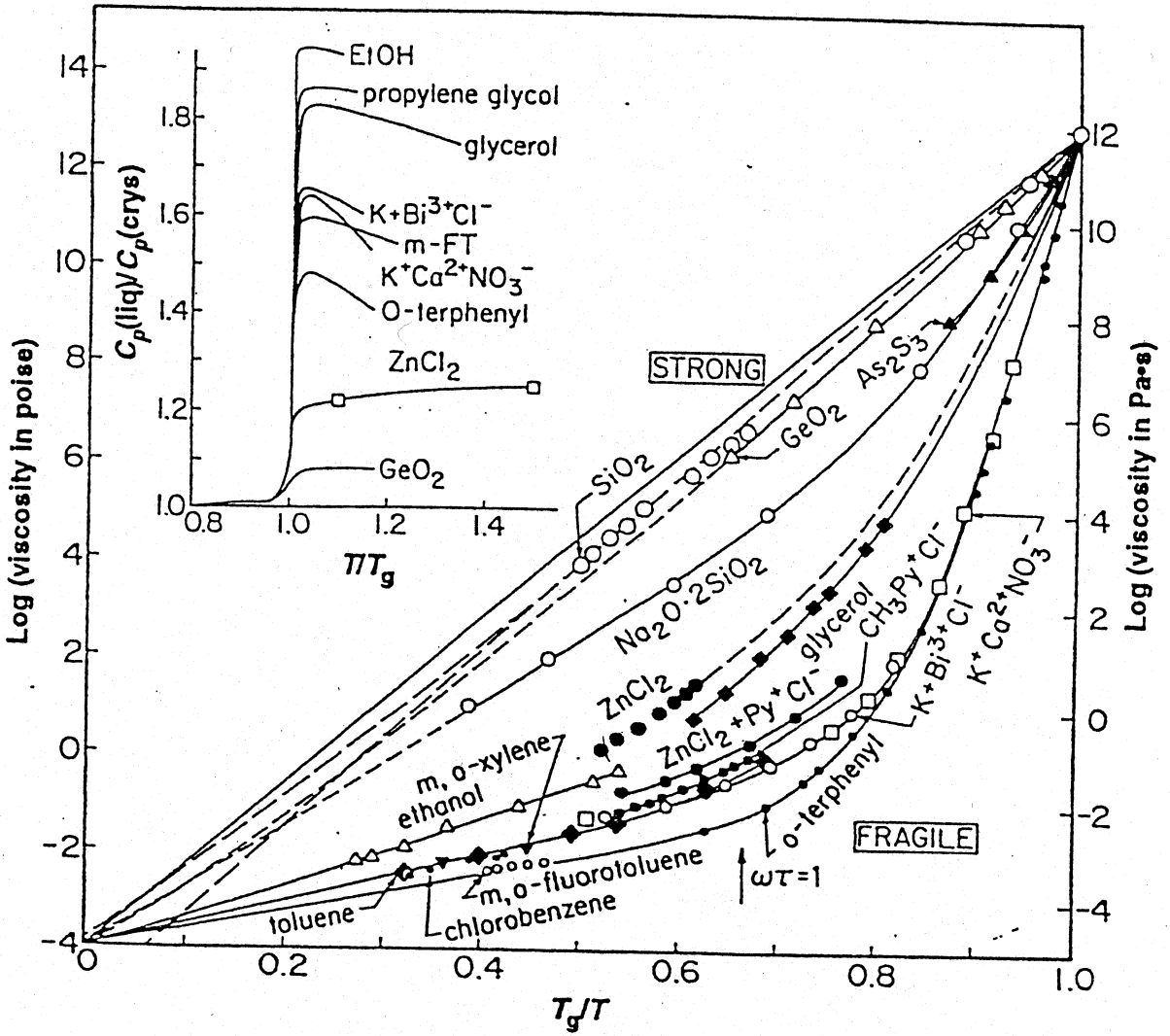

Fig. 13

Arrhenius plots of the viscosity data scaled by values of T_g from Fig. 3 and other sources showing the "strong-fragile" pattern of liquid behavior on which the liquid's classification of the same name is based. As shown in the insert, the jump in C_p at T_g is generally large for the fragile liquids and small for strong liquids, although there are a number of exceptions, particularly when hydrogen bonding is present.

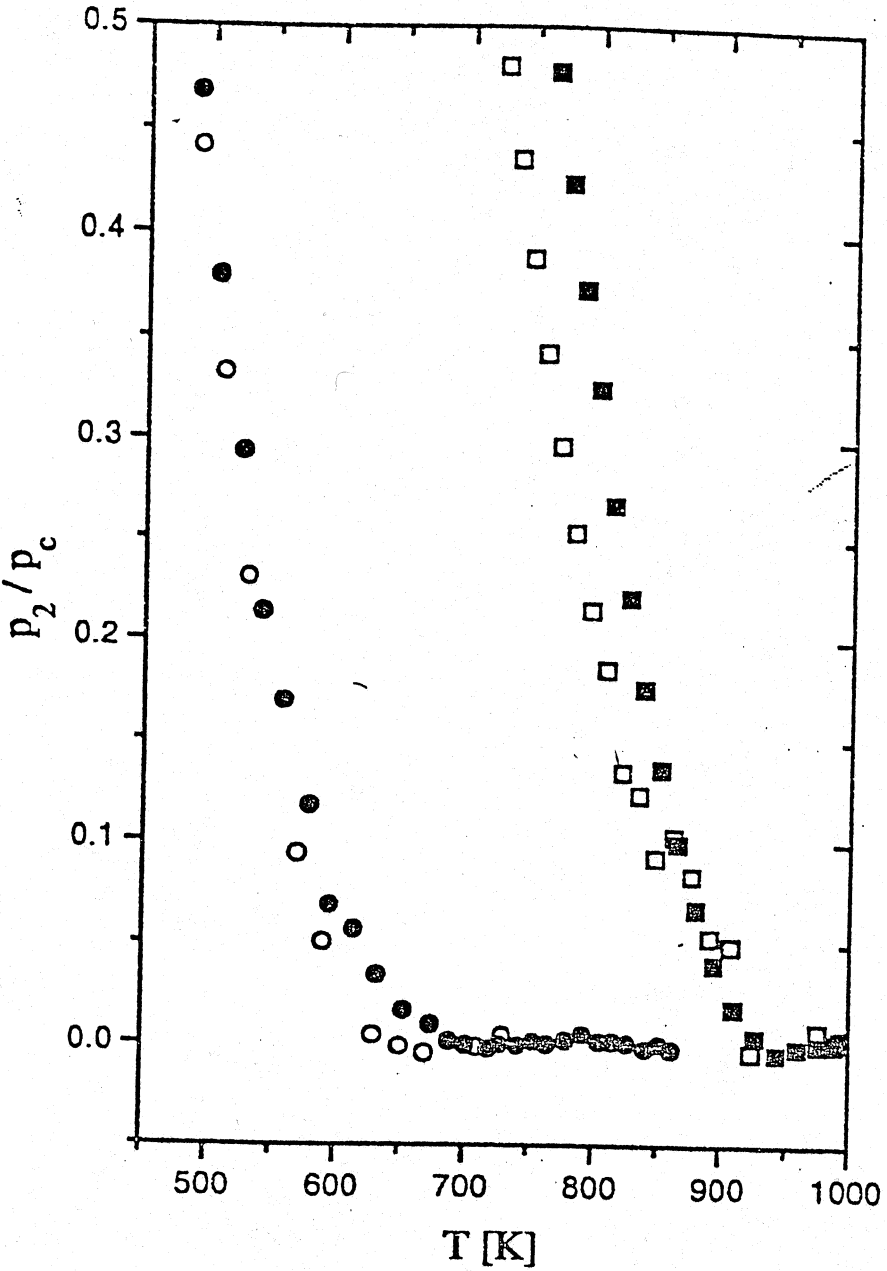

Fig. 15 Deviations from the 'fluid-phase' conductivity and fluidity of the effective conductivity $(\sigma_1 - \sigma_{\text{eff}})/\sigma_1 = p_2(T)/p_c'$ (empty symbols) and fluidity $(\varphi_1 - \varphi_{\text{eff}})/\varphi_1 = p_2(T)/p_c''$ (filled symbols) as functions of temperature. Circles correspond to $Ca_2Rb_3(NO_3)_7$ and squares to ZBLAN20 data.

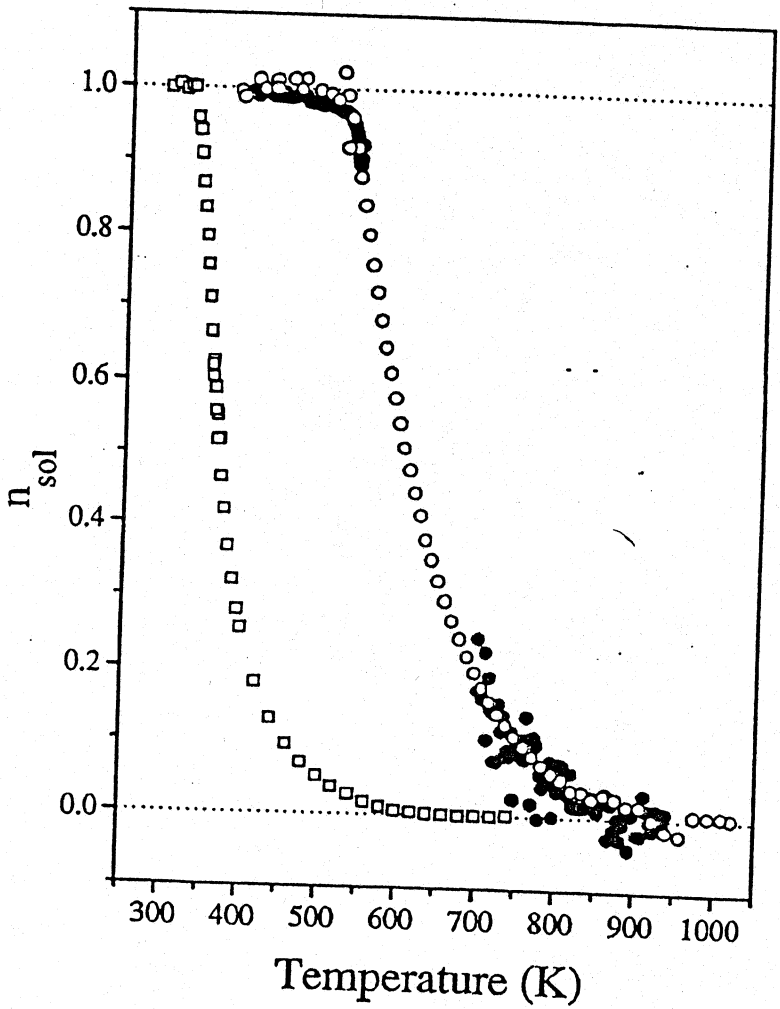

Fig. 16 The calculated volume fraction n_{sol} of the solid clusters in $Ca_2K_3(NO_3)_5$ (squares) and ZBLAN20 (circles) glass forming melts as a function of the temperature. Solid symbols are obtained from the density data, open symbols correspond to the resistivity data.